frontiers | Frontiers in Earth Science

TYPE Original Research
PUBLISHED 23 September 2022
DOI 10.3389/feart.2022.944549

OPEN ACCESS

EDITED BY
Yunhui Zhang,
Southwest Jiaotong University, China

REVIEWED BY
Huangsong Pan,
Southeast University, China
Zuosen Luo,
China Three Gorges University, China

*CORRESPONDENCE
Zuan Pei,
peizuan@cdut.edu.cn

SPECIALTY SECTION
This article was submitted to Geohazards and Georisks, a section of the journal Frontiers in Earth Science

RECEIVED 15 May 2022
ACCEPTED 31 August 2022
PUBLISHED 23 September 2022

CITATION
Yang H, Pei Z, He Z, Lei J and Xia X (2022), An empirical model for the travel distance prediction of deflection-type rock avalanches in the wenchuan earthquake area.
Front. Earth Sci. 10:944549.
doi: 10.3389/feart.2022.944549

An empirical model for the travel distance prediction of deflection-type rock avalanches in the wenchuan earthquake area

Hailong Yang[1], Zuan Pei[1]*, Zhihao He[2], Jin Lei[1] and Xiaotian Xia[3]

[1]State Key Laboratory of Geohazard Prevention and Geoenvironment Protection, Chengdu University of Technology, Chengdu, China, [2]School of Emergency Management, Xihua University, Chengdu, China, [3]Northwest Bureau of China Metallurgical Geology Bureau, Xi'an, China

Travel distance is a significant indicator for evaluating the mobility of rock avalanches and is usually used to identify the approximate delineation of potentially endangered regions. The deflection-type rock avalanche is a typical laterally confined rock avalanche and is characterized by obvious changes in the travel path. In this study, we selected deflection-type rock avalanches that occurred in the Wenchuan earthquake area as the research object and statistically analyzed 54 rock avalanches collected from the literature. Multiple linear regression of the logarithm of the ratio of slope height to travel distance (h/L) versus the logarithm of other parameters was developed to obtain a best-fit empirical model for the travel distance prediction of deflection-type rock avalanches. The validity of the proposed empirical model was verified by the satisfactory agreement between observations and predictions. Moreover, the sensitivity of local topographic parameters on the mobility of deflection-type rock avalanches is also discussed using regression analysis.

KEYWORDS

rock avalanche, deflection-type, travel distance, empirical model, local topography

1 Introduction

Rock avalanches are extremely rapid mass flows following the fragmentation of large rockslides or rockfalls (Hungr et al., 2014; Knapp and Krautblater, 2020; Mitchell et al., 2020). In the recent 2 decades, numerous typical rock avalanches have struck the southwestern mountain area of China, such as Touzhai rock avalanches (Yang et al., 2017), Guanling landslide (Kang et al., 2017), Chenjiaba landslide (Huang et al., 2017), Jiweishan landslide (Ge et al., 2019), Zhongbao landslide (Chen et al., 2021), etc., Due to their extremely high mobility (Ge et al., 2020a; Lin et al., 2022), they can travel unexpectedly long distances along different topographies (Hsu 1975; Ge et al., 2019), which always cause huge destructiveness to local residents and property in mountainous regions (Mitchell et al., 2019; Liu et al., 2021a).

The term "Fahrböschung" was first proposed by Heim (1932) in Elm landslide survey, and was used to measure the mobility of rock avalanches. A previous study revealed the inverse

relationship between the Fahrböschung values and volumes of rock avalanches (Strom et al., 2019; Mitchell et al., 2020). Thus, large rock avalanches are considered more mobile (Liu et al., 2021a). The travel distance, also called the runout distance, is another significant consideration for evaluating the mobility of rock avalanches. Since the famous Elm landslide event in 1881, the rapid long-travel distance rock avalanche harvest attention to continuously increasing interest from the scientists (e.g., Hsu 1975; Hungr and Evans 2004), which motivates further study to better estimate the mobility of these events. Moreover, travel distance is usually used to identify the rough delineation of potentially endangered regions (Hattanji and Moriwaki 2009). Therefore, it also has significance in the risk assessment of rock avalanches.

Previous studies have revealed that the mobility of rock avalanches is strongly affected by the local topography (Ge et al., 2020b; Liu et al., 2021a). The local topography along the travel path of rock avalanches mainly includes three basic confinement types: laterally confined, unconfined and frontally confined (Strom et al., 2019), also called valley, open and blocked topography (Zhang and Yin 2013). Laterally confined rock avalanches often move down a narrow or broad valley due to the constraint of the valley slopes of lateral mountains (Liu et al., 2021a), and their travel path usually undergoes obvious changes. The deflection angle, also known as impact angle (Ge et al., 2020b), is defined as the acute angle between the initial motion direction of the rock avalanches and the valley extension direction in the horizontal plan (Figure 1), which is used to describe the change in the travel path (Fan et al., 2015). According to the size of the deflection angle, the laterally confined rock avalanches can be further divided into two types, that is, deflection-type and channelized rock avalanches. The Wenjia gully rock avalanches triggered by the Wenchuan earthquake are striking examples of deflection-type rock avalanches. It underwent multiple changes in its travel path (Tang et al., 2012; Kang et al., 2021) and caused more than 50 people to lose their lives (Zhang et al., 2013, 2016). However, the effects of various topographical parameters on the mobility of deflection-type rock avalanches are still unclear at present.

Although the Wenchuan earthquake was over 10 years ago, it provided enormous amount of unstable slope for the post-earthquake hazards, such as the rainfall-induced Sanxicun landslide (Gao et al., 2017) and Xinmo rock avalanches (Huang et al., 2019) that severely threaten dwellings and infrastructures (Ding and Hu 2014). Therefore, the post-earthquake effect is still significant (Fan et al., 2018). Rock avalanches are the most common type of geological disasters in this region. Accordingly, the construction of a prediction model for the travel distance of rock avalanches is meaningful for the risk assessment of rock avalanches in this region (Zhan et al., 2017). Generally, travel distance prediction for rock avalanches is a complicated issue due to the great diversity in travel path materials (Liu et al., 2021a) and geotechnical parameters of mass flows (Qiu et al., 2018). The empirical prediction model, which avoids the usage of uncertain and highly variable parameters, provides a practical method (Qiu et al., 2018). Therefore, it has been widely applied to preliminary assessments of the travel distance of rock avalanches (e.g., Guo et al., 2014; Zhan et al., 2017; Strom et al., 2019; Mitchell et al., 2020). In the present study, the deflection-type rock avalanche was selected as the research object. A multiple linear regression model of the logarithm of h/L versus the logarithm of other parameters was developed to obtain a best-fit empirical model for the travel distance prediction of deflection-type rock avalanches, which provides a useful tool for the preliminary prediction of the potential threat range of such rock avalanches in the Wenchuan earthquake area. In addition, the effects of local topography on the mobility of deflection-type rock avalanches are further discussed.

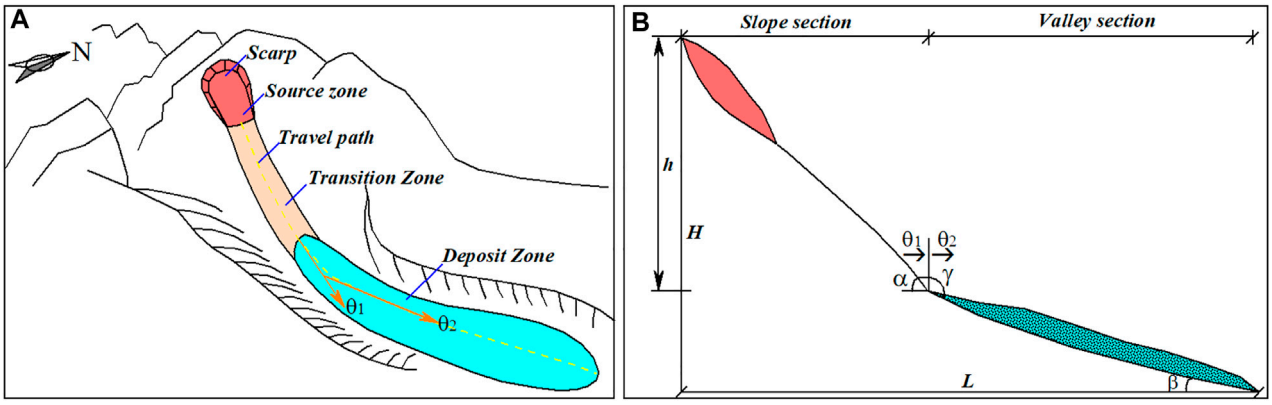

FIGURE 1
(A) Plane sketch of the deflected-type rock avalanches (θ_1 is refers to the initial motion direction of the rock avalanches, and θ_2 is refers to the valley extension direction); **(B)** Schematic diagram of local topography longitudinal section along the direction of motion path showing the main local topographic parameters of the deflection-type rock avalanches consist of the slope angle (α), channel angle (β), slope height (h), deflection angle (θ), slope transition angle (γ) and fall height (H).

2 Rock avalanche database

The Tibetan Plateau, located at the junction of Indian and Asian plates, has undergone long–term and complex tectonic activities since the late Mesozoic (Zhang et al., 2022). Longmen Shan Mountain (LMS) Orogenic Zone belongs to southeastern region of the Tibetan Plateau, and is one of the most intense areas in mainland China on crustal deformation characterized by frequent large earthquakes (Wang et al., 2014). Rock slides and collapses are the main types of earthquake disasters in LMS Orogenic Zone, and each strong earthquake usually causes massive rockslides and collapses in this region. For example, the tectonic uplift caused by the Wenchuan earthquake changed the slope gradient instantly (Li et al., 2014) and triggered more than 60,000 rock slides over an elliptical area of approximately 44,000 km^2 along the fault rupture zone (Liu et al., 2021b), which directly led to approximately 20,000 deaths.

The co-seismic landslides triggered by Wenchuan earthquake provides a rich database for landslide statistical analysis. Therefore, we compile three databases of rock avalanches in this study (see Tables 1, 2, 3). The collected data is associated with the Wenchuan earthquake area. As shown in Figure 2, the rock avalanches listed in the databases are distributed on the surface rupture zone with northeast-trending between the Sichuan Basin and the Tibetan Plateau. Database one consists of 22 rock avalanches collected from the literature (Table 1). It was used to validate the general applicability of the empirical model proposed in this paper in travel distance prediction. Database two consists of 54 deflected-type rock avalanches (Table 2). The volumes of these rock avalanches ranged from 2.6 to 1996 × 10^4 m^3, with travel distances between 0.13 and 2.40 km (Table 2). Deflected-type rock avalanches were used to develop an empirical model for travel distance prediction. In addition, as shown in Table 3, database three consisting of 10 deflected-type rock avalanches was applied to verify the validity of the presented model. The data in database three were collected based on remote sensing interpretation and field investigation on Subaohe river Basins, Beichuan county in the Wenchuan earthquake area (see inset of Figure 2).

TABLE 1 The database of laterally confined rock avalanches.

No	Landslide name	Landslide volume V (10^4m^3)	Slope angle α (°)	Channel angle β (°)	Fall height H (m)	Observed travel distance L observed (m)	Predicted travel distance L predicted (m)	Estimation errors
1	WenjiaGully	5,000	26	7	1,320	4,000	4,686	17.14(%)
2	HongshiGully	1,341	37	17	1,040	2,700	1999	25.95(%)
3	Xiaojiashan 1#	781	48	24	930	1,350	1,246	7.72(%)
4	NiumianGully	750	32	13	800	2,640	1887	28.51(%)
5	LiqiGully	536	37	12	650	1,500	1,434	4.39(%)
6	Caocaoping	534	31	17	580	1,340	1,247	6.93(%)
7	HuoshiGully	468	38	17	700	1,320	1,305	1.16(%)
8	Shibangou	450	34	9	650	1800	1705	5.29(%)
9	Xiejiadianzi	400	34	15	720	1,600	1,523	4.84(%)
10	DashuiGully	315	30	17	560	1,400	1,218	12.97(%)
11	Changping	284	37	16	500	1,200	972	19.04(%)
12	Xiaomuling	274	45	26	710	1,025	955	6.86(%)
13	Dawan	248	28	20	480	1,000	1,015	1.49(%)
14	Xiaojiashan 2#	239	44	20	650	1,135	1,000	11.87(%)
15	Shicouzi	192	30	26	640	1,200	1,141	4.92(%)
16	Changtan	164	33	25	1,050	1,650	1771	7.34(%)
17	Zhangzhengbo	92	29	15	320	800	741	7.42(%)
18	Dujiayan	86	33	17	400	880	804	8.63(%)
19	Madiping	86	27	31	395	740	687	7.13(%)
20	Yandiaowo	82	30	26	390	800	691	13.66(%)
21	ChuangziGully	82	35	15	295	670	604	9.85(%)
22	Waqianshan	56	24	18	250	620	598	3.59(%)

Note: The database collected from the literature of Zhan et al. (2017).

TABLE 2 Data of various parameters of deflected-type rock avalanches.

No	Landslide name	Landslide volume V (10^4m^3)	Slope height h (m)	Slope angle α (°)	Channel angle β (°)	Deflection angle θ (°)	Transition angle γ (°)	Fall height H (m)	Observed travel distance L observed (m)	Predicted travel distance L predicted (m)	Estimation errors
1	Anzi	2.6	57	33	31	52	178	107	171	157	8.19(%)
2	Daihuashan	2.8	38	32	31	48	179	78	130	122	6.35(%)
3	Majiahe	2.8	90	46	36	43	170	145	163	153	6.22(%)
4	Jiulong Gully 1#	2.9	81	29	28	65	179	137	251	246	1.80(%)
5	Laohuzui Gully 1#	3.3	154	37	27	43	167	221	335	363	13.11(%)
6	Siping	4	179	38	25	27	169	268	418	328	11.80(%)
7	Muguayuan	7.2	117	30	19	35	173	176	372	271	2.94(%)
8	Tianping Village	7.6	112	37	30	40	172	189	279	362	8.93(%)
9	Huangnigang	8.2	175	43	35	23	165	321	398	271	14.04(%)
10	Pianqiaozi	8.8	153	35	19	36	168	205	372	409	7.21(%)
11	Wujibao	9.3	112	32	17	71	178	153	315	529	4.03(%)
12	Zaojiaowan Gully 1#	13.1	217	42	30	64	172	335	441	376	5.99(%)
13	Jinxi Gully	14.6	138	49	40	30	162	297	312	455	4.52(%)
14	Jiulong Gully 2#	16.5	198	37	35	52	162	403	551	380	26.70(%)
15	Qilangmiao	19.5	113	31	23	20	172	201	400	937	30.02(%)
16	Chuangzi Gully 2#	20.1	203	39	21	37	171	274	435	828	15.79(%)
17	Yangjiayan	25.4	164	41	23	27	160	304	518	639	7.08(%)
18	Xiaowan	20.4	342	31	23	42	170	409	721	945	16.33(%)
19	Shanshulin	27.9	340	34	25	66	169	433	715	651	10.34(%)
20	Huangjiabacun	32	282	38	18	45	168	362	597	493	0.37(%)
21	Zaojiaowan Gully 2#	37.4	428	39	29	56	162	582	812	648	22.48(%)
22	Pingshang	38.2	215	31	20	44	161	300	590	650	6.92(%)
23	Yuzixi	40	212	40	28	56	177	342	495	931	25.32(%)
24	Huangbashi	44.7	275	47	23	62	179	414	579	542	7.39(%)
25	Liushuping	34.9	200	26	8	57	149	218	529	810	6.37(%)

(Continued on following page)

10.3389/feart.2022.944549

TABLE 2 (*Continued*) Data of various parameters of deflected-type rock avalanches.

No	Landslide name	Landslide volume V (10^4m^3)	Slope height h (m)	Slope angle α (°)	Channel angle β (°)	Deflection angle θ (°)	Transition angle γ (°)	Fall height H (m)	Observed travel distance L observed (m)	Predicted travel distance L predicted (m)	Estimation errors
26	Xingziping	52.6	284	41	22	37	172	396	608	749	14.05(%)
27	Laoshuzui Gully 2#	58.7	281	35	32	21	166	491	743	669	15.87(%)
28	Muhongping	85.7	171	28	21	47	170	403	931	957	25.38(%)
29	Laojiaozi Gully	65.6	139	27	26	85	161	259	505	693	14.61(%)
30	Daozaiqiao	67.3	399	40	9	70	174	464	865	494	26.92(%)
31	Weiziping	68.6	157	22	14	28	162	222	657	519	5.22(%)
32	Pujia Gully	71.8	239	35	21	50	155	413	795	881	7.31(%)
33	Fuyan Gully	51.9	385	38	28	40	171	530	763	718	3.80(%)
34	Zhangjiaping	74.7	286	39	20	50	154	379	605	699	1.96(%)
35	Zhaojiashan	78.4	94	22	16	30	157	223	676	876	31.66(%)
36	Chuangzi Gully 1#	90.9	178	34	16	60	175	261	548	1,280	8.97(%)
37	Longwan Village	102.1	268	32	29	55	168	489	830	462	42.99(%)
38	Zhuanwan	113.3	498	48	23	69	165	713	950	1,136	26.94(%)
39	Qinglong Village	118.9	133	20	11	37	163	194	692	1,053	26.51(%)
40	Linjiashan	120.6	258	32	6	80	167	285	686	1,089	23.76(%)
41	Changheba	120.9	354	41	18	30	167	439	665	1,396	28.58(%)
42	Maochongshan	130.6	392	37	22	33	162	566	938	1,351	18.28(%)
43	Pengjiashan	142.1	316	29	24	24	156	591	1,175	1818	25.82(%)
44	Baiguoshu	161.8	104	26	14	50	158	255	811	1,465	28.51(%)
45	Hongmagong	169.6	320	29	14	45	150	403	895	2039	15.05(%)
46	Fengyanzi	192.1	289	30	13	31	170	365	832	312	6.88(%)
47	Yinshan Gully	224.1	363	38	25	30	164	556	880	360	3.34(%)
48	Baishu Gully	280.4	331	39	22	43	171	622	1,147	264	15.44(%)
49	Dongxi Gully	350.6	360	28	15	55	156	471	1,086	492	15.11(%)
50	Mianjiaoping	629.2	461	38	20	64	173	660	1,142	659	29.24(%)
51	Haixin Gully	969.8	720	40	16	80	177	891	1,445	939	13.17(%)
52	Donghekou	1,500	560	35	5	27	165	700	2,400	1,097	16.92(%)
53	Woqian	1,602.3	375	30	8	75	163	575	2050	950	17.16(%)
54	Shuimo Gully	1996	578	34	16	50	162	754	2000	2,182	9.12(%)

Note: The database collected from the literature of Fan et al. (2015).

10.3389/feart.2022.944549

TABLE 3 Database of deflection-type rock avalanches used for applicability verification of the improved empirical model.

No.	Landslide name	Landslide volume V (10^4m^3)	Slope height h (m)	Slope angle α (°)	Channel angle β (°)	Deflection angle θ (°)	Observed travel distance L observed (m)	Predicted travel distance L predicted (m)	Estimation errors
1	Tianba	0.74	95	30	27	51	200	223	11.50(%)
2	Yangjiayan	18.60	119	35	23	25	574	334	41.81(%)
3	Shuicheping	4.44	74	28	23	14	354	242	31.64(%)
4	Liujiaping	1.26	49	28	20	45	148	131	11.49(%)
5	Huangjiashan	3.31	109	34	30	33	228	276	21.05(%)
6	Yinbashi	99.19	257	32	20	21	878	882	0.46(%)
7	Shaojiashan	1.49	212	35	28	13	368	432	17.39(%)
8	Tianping	8.87	91	30	24	28	381	290	23.88(%)
9	Chenshan	0.24	27	24	17	63	105	69	34.29(%)
10	Yuanxing	2.98	114	35	33	41	268	287	7.09(%)

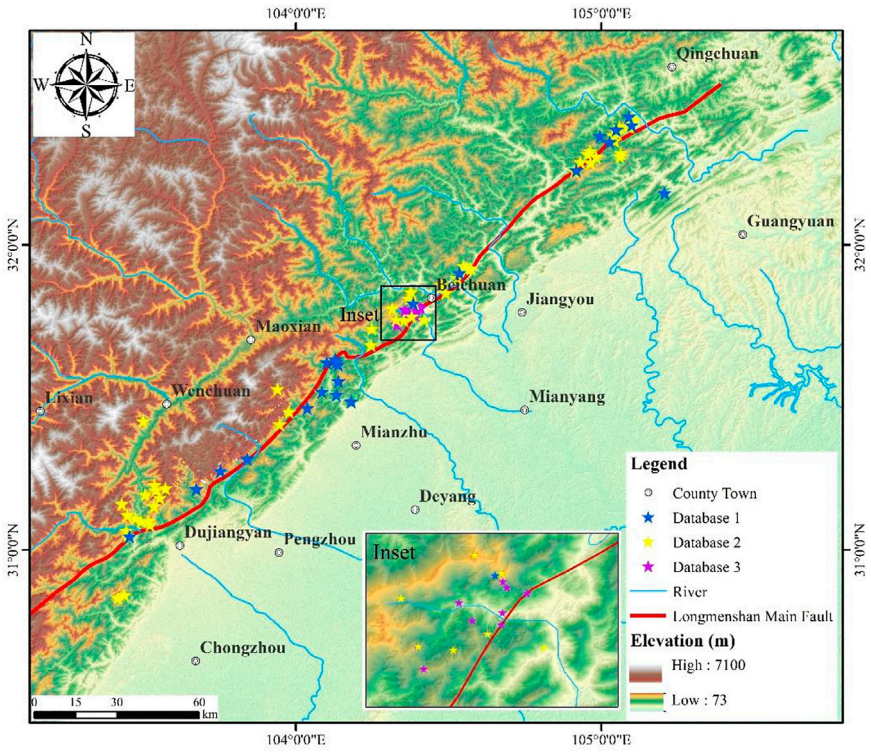

FIGURE 2
The locations of rock avalanches in the Wenchuan earthquake area collected in three databases.

3 Method

3.1 Relevant parameters

The local morphology of a deflection-type rock avalanche can be divided into two sections consisting of slope and valley sections (Figure 1A). The terms and notations of the deflection-type rock avalanches are shown in Figure 1B. The slope angle (denoted as α) refers to the average inclination from the slope toe to the top of the scarp (Qiu et al., 2018). The channel angle (denoted as β) refers to the average inclination of the sectional valley (Zhan et al., 2017). The topographic relief change between slope and valley is defined as the

slope transition angle (denoted as γ) (Guo et al., 2014). The fall height (denoted as H) is the vertical distance from the top of the scarp to the front end of the deposit (Basharat et al., 2015). The slope height (denoted as h) refers to the vertical distance from the top of the scarp to the slope toe. The symbol θ_1 is used to represent the initial motion direction of the rock avalanches, whereas the symbol θ_2 is used to represent the valley extension direction. The deflection angle (denoted as θ) is the acute angle between θ_1 and θ_2 (Fan et al., 2015). Therefore, the main local topographic parameters of the deflection-type rock avalanches consist of the slope angle (α), channel angle (β), slope height (h), deflection angle (θ), slope transition angle (γ) and fall height (H).

3.2 Empirical model

Empirical-statistical methods have been used as common tools to study the mobility of rock avalanches (Zhan et al., 2017). In reference to existed study (e.g., Heim 1932; Hsu 1975; Qiu et al., 2018; Zheng et al., 2018), although there are many empirical models available for travel distance prediction of rock avalanches, they can be summarized into just three categories, as shown in Eqs 1, 2, 3. However, Eqs 1, 2 only describe the simple statistical relationships between mobility parameters and landslide volume, while Eq. 3-1 proposed by Zheng et al. (2018) and Eq. 3-2 proposed in this paper have much more physical significance. Therefore, Eq. 3 was selected as the empirical model for travel distance prediction.

$$L(V) = \lambda_0 V^{\lambda_1}, \tag{1}$$

$$\frac{H}{L}(V) = \gamma_0 V^{\gamma_1}, \tag{2}$$

$$L(VH) = \eta_0 (VH)^{0.25}, \tag{3-1}$$

$$\frac{H}{L}(V) = \chi_0 \left(V^{1/3} H^{-1}\right)^{\chi_1}, \tag{3-2}$$

where the L is the indicator variable, H is the fall height, V is the landslide volume, and λ_0, λ_1, γ_0, γ_1, η_0, χ_0 and χ_1 are the corresponding regression coefficients.

The mobility of rock avalanches is affected by several influential factors (Guo et al., 2014). Hence, some scholars have aimed to introduce more quantifiable influential factors in empirical models to improve the prediction accuracy of travel distance (e.g., Finlay et al., 1999; Guo et al., 2014; Zhan et al., 2017; Qiu et al., 2018). The local topography is an important factor influencing the mobility of rock avalanches (Liu et al., 2021a). Therefore, after introducing the main topographic parameters in Eq. 3-1 and Eq. 3-2, the empirical model can be expressed as Eq. 4. The linear regression model on the logarithmic transform of the variables was conducted under the assumption of linear association, in which logarithmic transformation of the variables is equivalent to a power law consistent with the existing research (Mitchell et al., 2020).

$$\log L = \beta_0 + \beta_1 \log (VH)^{0.25} + \beta_2 \log C_1 + \beta_3 \log C_2 + \ldots + \beta_{n+1} \log C_n + \varepsilon, \tag{4-1}$$

$$\log\left(\frac{H}{L}\right) = \beta_0 + \beta_1 \log\left(V^{1/3} H^{-1}\right) + \beta_2 \log C_1 + \beta_3 \log C_2 + \ldots + \beta_{n+1} \log C_n + \varepsilon, \tag{4-2}$$

where log is the logarithm of 10, L is the travel distance, H is the fall height, V is the landslide volume, C_i (i = 1, 2, 3..., n + 1) are the indicator variables of topographical parameters, β_i (i = 1, 2, 3..., n + 1) are the regression coefficients and ε is the residual error, which is assumed to be normally distributed with zero mean (Mitchell et al., 2020).

As shown in Eqs 5, 6, the mean absolute percentage error, hereinafter referred to as *MAPE* (Armstrong and Collopy 1992), and the Theil inequality coefficient, hereinafter referred to as *TIC* (Leuthold 1975), can be used to evaluate the prediction accuracy of the empirical model for the travel distance prediction of deflected-type rock avalanches.

$$MAPE = \frac{1}{\mathrm{n}} \sum_{1}^{n} \left| \frac{p_i - A_i}{A_i} \right|, \tag{5}$$

$$TIC = \frac{\sqrt{1/\mathrm{n} \sum_{1}^{n} (p_i - A_i)^2}}{\sqrt{1/\mathrm{n} \sum_{1}^{n} p_i^2} + \sqrt{1/\mathrm{n} \sum_{1}^{n} A_i^2}}, \tag{6}$$

where p_i and A_i refer to predictions and actual observations of travel distance, respectively. A smaller MAPE or TIC value indicates that the empirical models are more accurate in predicting the travel distance of rock avalanches (Qiu et al., 2018).

4 Results and validation

4.1 General applicability validation

The parameters of 22 rock avalanches listed in the test database one consist of landslide volume (V), fall height (H), slope angle (α) and channel angle (β). Therefore, the slope angle (α) and channel angle (β) were considered in Eq. 4. Based on the multivariate regression method, the best-fit regression equation for travel distance prediction was derived from the dataset of Table 1 (see Eq. 7).

$$L = e^{2.312} (\tan\alpha)^{-0.308} (\tan\beta)^{-0.817} (VH)^{0.25}, \tag{7-1}$$

$$\frac{H}{L} = e^{0.1247} (\tan\alpha)^{0.5211} (\tan\beta)^{0.4017} \left(V^{1/3} H^{-1}\right)^{-0.0184}. \tag{7-2}$$

The regression results show that correlation coefficients are 0.39 and 0.77 for Eq. 7-1 and Eq. 7-2. Meanwhile, the p value of Eq. 7-2 is 0.013 and is less than that of Eq. 7-1, which indicates that the

overall regression of Eq. 7-2 satisfies higher statistical significance level. In addition, the residual plots illustrate normality, constant variance and absence of trends in the residuals (Figure 3), which shows that the selection of Eq. 7-2 as empirical prediction model for travel distance is more reasonable. To further validate Eq. 7-2, we list the estimation errors ($|L_{predicted} - L_{observed}|/L_{observed} \times 100\%$) of 22 rock avalanches in Table 1. Most of the estimation errors are less than 10%, which indicates that the travel distance of most rock avalanches is predicted accurately. Therefore, the empirical model (Eq. 4-2) has good applicability in travel distance prediction for rock avalanches.

4.2 Travel distance prediction for the deflection-type rock avalanches

For the travel distance prediction of deflected-type rock avalanches, four characteristic parameters of local topography, including α, β, θ and γ, were considered in the empirical model (Eq. 4-2), and the best-fit multivariate regression model (Eq. 8) was obtained based on the regression analysis of the database of deflection-type rock avalanches, which is as follows:

$$\frac{H}{L} = e^{0.1839} (tan\,\alpha)^{0.6181} (tan\,\beta)^{0.2586} (tan\,\theta)^{0.0318} (sin\,\gamma)^{0.0063} (V^{1/3}H^{-1})^{-0.0480}. \quad (8)$$

The histogram of relative frequency (Figure 4A) shows that log(H/L) regression residuals approximately fit a normal distribution, which supports the normality assumption. The plot of residuals shows an absence of trends (Figure 4B), indicating the independence in residuals and its homogeneity of variance (Liu et al., 2021a). Moreover, the p value (0.0062) of the significance test of Eq. 8 is less than 0.05, indicating that the regression relationship is statistically significant at a 95% confidence level. The regression results indicate that the best-fit multivariate regression model (Eq. 8) has a high correlation coefficient (R^2=0.93) and a strong statistical significance level.

However, some uncertain parameters were included in the empirical model, resulting in limitations in its practical engineering application. For example, the fall height H is an uncertain parameter before the occurrence of rock avalanches. Some scholars have introduced the height of the source area (h') or slope height (h) to replace the fall height (H) in empirical models (e.g., Zhan et al., 2017; Fan et al., 2015). However, the slope height (h) has much more physical significance because it implies the preimpact potential energy of rock avalanches (Guo et al., 2014). In addition, the channel angle (β) is closely related to the slope angle (α) and slope transition angle (γ). Therefore, the slope height (h), landslide volume (V), slope angle (α), slope transition angle (γ) and deflection angle (θ) were considered in the improved empirical model (see Eq. 9). Eventually, the best-fit regression equation was derived from the dataset of Table 2, as shown in Eq. 9:

$$h/L = e\,0.1621\,(tan\,\alpha)^{0.6958} (\tan\theta)^{0.0727} (\sin\gamma)^{0.0865} (V^{1/3}h^{-1})^{-0.1206} \quad (9)$$

The adjusted coefficient of determination R^2 is relatively high, with a value of 0.7, which indicates a good correlation between h/L and the landslide volume, slope height and the three characteristic parameters of local topography. This high R^2 indicates the small scatter in the data points about the regression line. In addition, the histogram of relative frequency (Figure 5A) shows that the regression residuals of log h/L also follow an approximate normal distribution. Meanwhile, the plot of residuals (Figure 5B) demonstrates the independence in residuals and homogeneity of variance. The p value (0.036) of the significance test for Eq. 9 is less than 0.05,

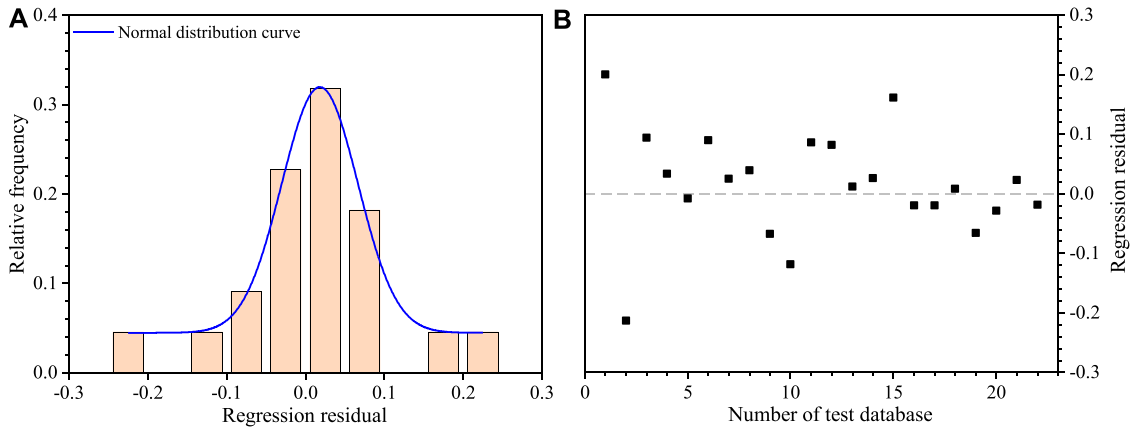

FIGURE 3
The regression analysis results of Eq. 7-2 based on the test database of 22 channelized rock avalanches: **(A)** Histogram of the relative frequency of the log(H/L) regression residuals. **(B)** Plot of regression residuals of log(H/L).

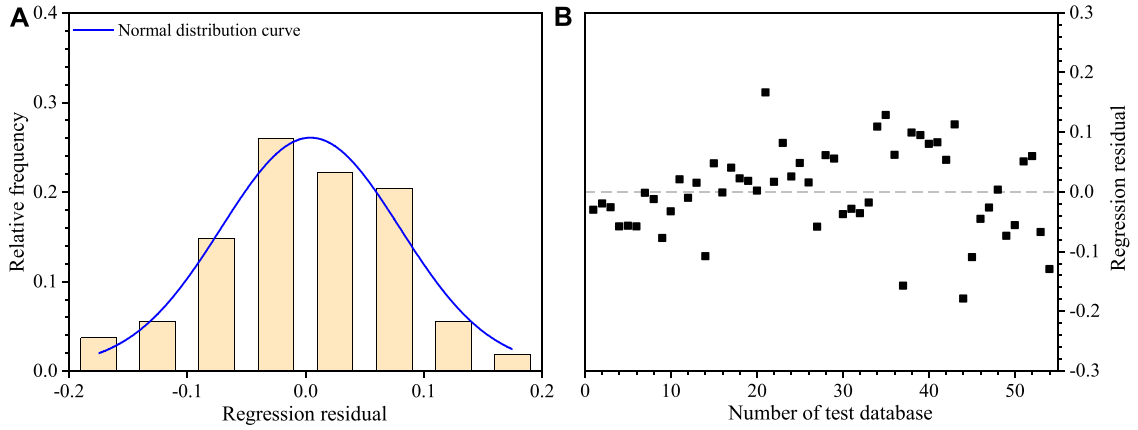

FIGURE 4
The regression analysis results of Eq. 8 based on the database of 54 deflected-type rock avalanches: **(A)** Histogram of the relative frequency of the log(H/L) regression residuals. **(B)** Plot of regression residuals of log(H/L).

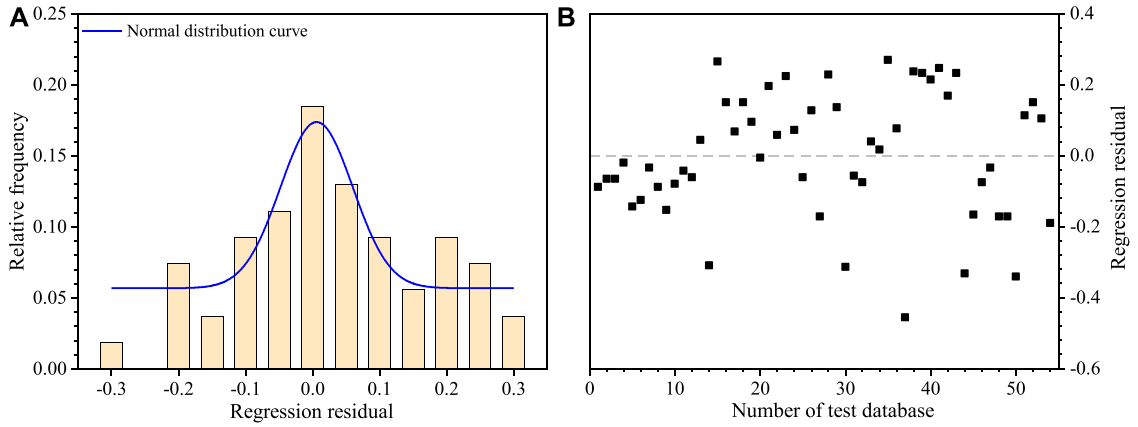

FIGURE 5
The regression analysis results of Eq. 9 based on the database of 54 deflected-type rock avalanches: **(A)** Histogram of the relative frequency of the log(h/L) regression residuals. **(B)** Plot of regression residuals of log(h/L).

indicating that this improved empirical model is also statistically significant at a 95% confidence level.

4.3 Applicability validation

The agreement between predictions and observations is usually used to evaluate the prediction accuracy of the empirical model (Qiu et al., 2018). Figure 6A compares the predicted travel distances estimated by Eq. 9 with the observed avalanches of 54 deflected-type rock avalanches. The predicted values of the samples are close to the observed values (Figure 6A). The estimation error results show that Eq. 9 has an average error of < 20% (Table 2). The self-verification results suggest that Eq. 9 is valid for most deflection-type rock avalanches (Figure 6A). The database of Table 3 is used to further discuss the validity of Eq. 9. The compared results between the observed and predicted travel distances of 10 deflected-type rock avalanches are depicted in Figure 6B. The analysis results of the estimation error show that the maximum error is 41.81%, the minimum error is 0.46% and the average error is approximately 20% (Table 3). Based on this, it can be determined that the improved empirical model (Eq. 9) achieves an acceptable prediction accuracy for the travel distance of deflected-type rock avalanches in the Wenchuan earthquake area.

5 Discussion

The H/L ratio is commonly used to study the mobility of rock avalanches in previous study (e.g., Qiu et al., 2018; Liu et al., 2021a).

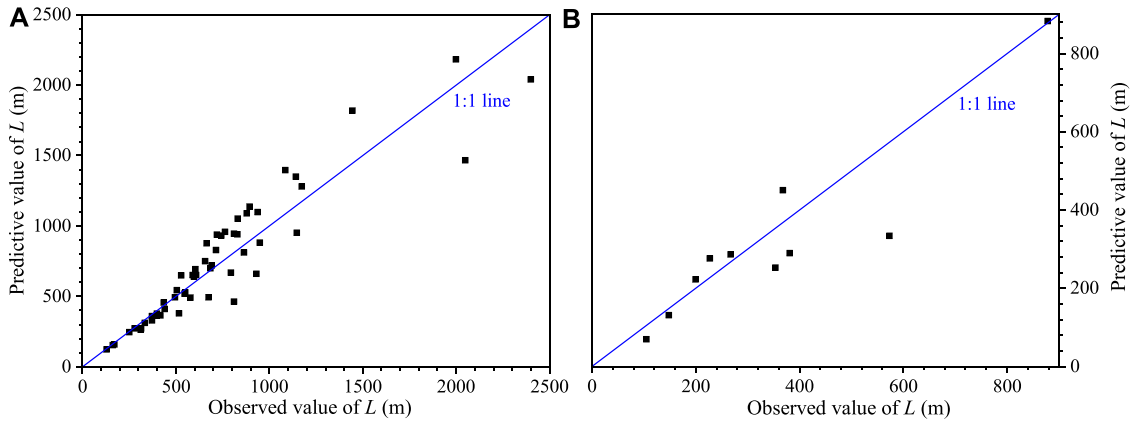

FIGURE 6
The comparison between the observed and predicted travel distances for Eq. 9: **(A)** Comparison results of 54 deflected-type rock avalanches; **(B)** comparison results of an independent validation dataset of 10 deflected-type rock avalanches.

Many studies have shown a negative correlation between the H/L ratio and the landslide volume, although the slope and intercept of its regressive relationship are varied (e.g., Hattanji and Moriwaki 2009; Qiu et al., 2018; Strom et al., 2019; Mitchell et al., 2020). In this study, we propose an alternative parameter, the h/L ratio, and the regression analysis results show that the h/L ratio decreases with an increasing landslide volume (V), suggesting the h/L ratio also can be used to evaluate the mobility of rock avalanches. Compared to H/L ratio, the h/L ratio is preferable as a measure of the travel distance prediction of rock avalanches due to the higher coefficient of determination of h. In addition, the simple linear regression of the logarithm of the h/L ratio plotted against the logarithm of $V^{1/3}/h$ also show a negative correlation, but the very low coefficient of determination R^2 (0.26) indicates that the simple linear regression is weak (Figure 7A). This finding may primarily be attributed to neglecting the effects of other influence factors, such as local topographic parameters, etc., As shown in Eq. 9, the multiple linear regression of the logarithm of h/L versus the logarithm of other parameters consisting of slope height (h), landslide volume (V), slope angle (α), deflection angle (θ) and slope transition angle (γ) has a high correlation coefficient (R^2=0.7) and strong statistical significance level. It can be concluded that the local topography plays an important role in the mobility of rock avalanches. Therefore, more consideration should be given to the influence of local topographic parameters in the empirical model for the travel distance prediction of deflection-type rock avalanches.

In previous study, the effects of local topography on rock avalanches' mobility have been constantly focus of attention by some authors who explored the variability in behaviour between the rock avalanches events of different local topography categories (e.g., Zhang and Yin, 2013; Liu et al., 2021a). However, the focus of this paper is the sensitivity analysis of different local topographic parameters to rock avalanches' mobility for a certain confinement type. Therefore, another three best-fit regression models, in which only two local topographic parameters are considered, were derived from the dataset of 54 deflected-type rock avalanches (Table 4). A comparison shows that the correlation coefficients for these three regression models are 0.52, 0.68, 0.67 respectively, which both lower than that of Eq. 9. This means that the travel distance predicted using three independent topographic variables performs better than the travel distance predicted using two independent variables. Additionally, MAPE and TIC values can directly reflect the effect of various topographic parameters on the mobility of deflected-type rock avalanches. The results show that the MAPE and TIC values calculated by Eq. 12 are the lowest, followed by the MAPE and TIC values calculated by Eq. 11. The MAPE and TIC values calculated by Eq. 10 are the highest. The results suggest that the prediction accuracy decreases in turn for Eqs 10–12. Hence, according to the MAPE and TIC values, it can be inferred that the order of sensitivity of the three independent topographic parameters on the mobility of deflected-type rock avalanches is as follows from large to small successively: $\alpha > \theta > \gamma$. This indicate that the slope angle (α) is predominant in the travel distance, which is reverse to the channelized rock avalanches. Previous study shows the slope angle (α) does not have a significant correlation with travel distance, whereas the channel angle (β) plays the dominating role in the travel distance of channelized rock avalanches (Zhan et al., 2017). Moreover, the sensitivity analysis results indicate that the mobility of deflected-type rock avalanches is also strongly dependent on the deflection angle (θ), which is different from channelized rock avalanches.

The positive correlation between travel distance and landslide volume of rock avalanches has been discussed in previous study (e.g., Budetta and De Riso 2004; Guo et al., 2014), and the predominant effects of landslide volume on mobility of rock avalanches was stressed. In this study, 54 deflected-type rock avalanches were divided into three categories, including large-scale ($V > 100 \times 10^4$ m^3), medium-scale ($10 \times 10^4 \leq V \leq 100 \times 10^4$ m^3) and

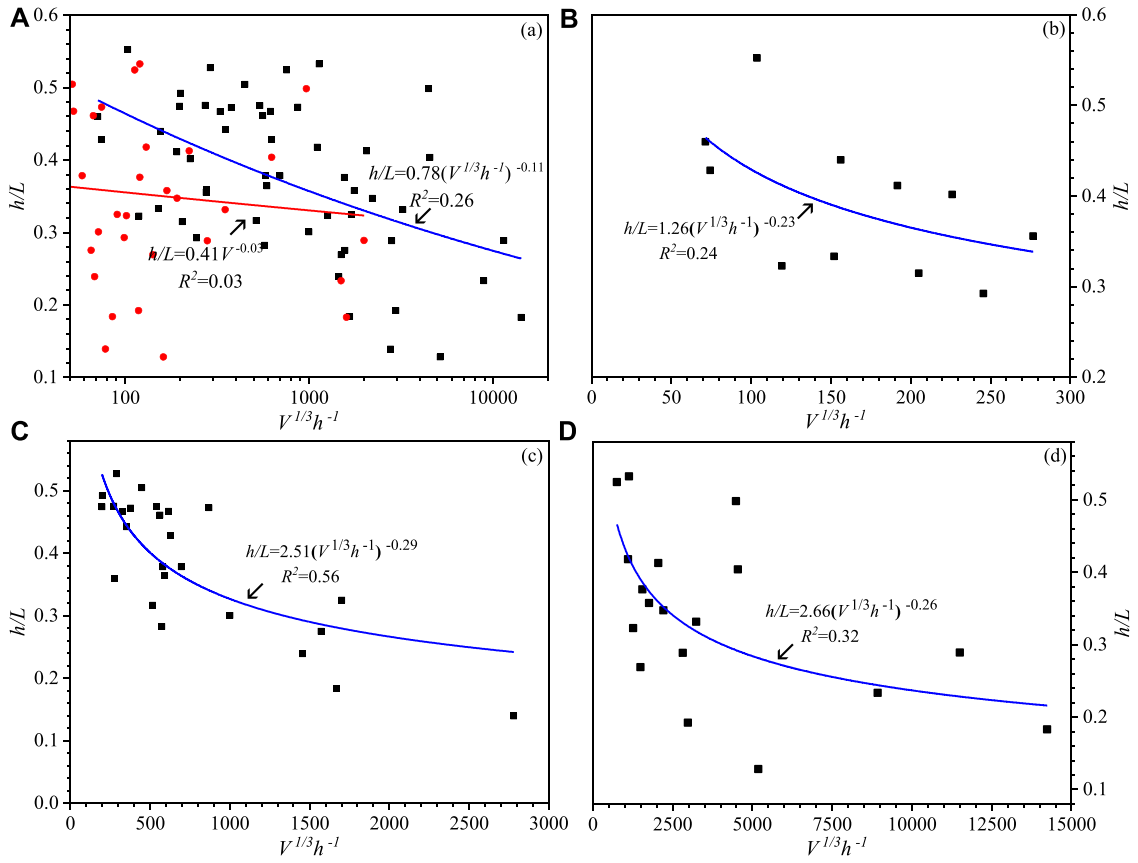

FIGURE 7
Simple linear regression of the logarithm of the *h*/*L* ratio predicted from the logarithm of $V^{1/3}/h$ or *V* without consideration of the local topography: **(A)** Regardless of the volume effect; **(B)** large-scale rock avalanches; **(C)** medium-scale rock avalanches; **(D)** small-scale rock avalanches.

TABLE 4 Comparison of the regression results for different empirical models using different independent topographic variables.

Equation	Intercept	Coefficients				R^2	*p*-value	Comments	MAPE (%)	TIC
		tanα	tanθ	sinγ	$V^{1/3}h^{-1}$					
Eq. 9	1.1760	0.6958	0.0727	0.0865	−0.1206	0.70	0.035	Good correlation	14.61	0.0194
Eq. 10	1.7153	—	0.0942	0.1905	−0.1902	0.52	0.05	Minor correlation	17.84	0.0281
Eq. 11	1.1026	0.7226	—	0.0777	−0.1104	0.68	0.038	Good correlation	16.57	0.0215
Eq. 12	0.8907	0.8361	0.0633	—	−0.0929	0.67	0.039	Good correlation	15.49	0.0196

small-scale (V <10 × 10^4 m^3) rock avalanches according to the landslide volume. The results show a lower significance level and correlation coefficients of the simple linear regressions of the logarithm of h/L versus the logarithm of $V^{1/3}/h$ for rock avalanches with different scales (Figures 7B–D). This indicate that the simple linear regressions between the logarithm of h/L ratio and logarithm of $V^{1/3}$/h is rather weak. However, the multiple linear regression models in which the local topographic parameters were considered (Eqs. 13–15) have higher significance levels and correlation coefficients (Table 5). The correlation coefficients in sequence from large to small corresponds to the regression models of small-, medium- and large-scale rock avalanches. In addition, the calculation results of MAPE and TIC show that the prediction accuracy from large to small corresponds to Eqs 13–15 (Table 5). This result suggests that the effect of local topography on the mobility of rock avalanches gradually decreases with increasing landslide scale. Therefore, we suggest that more quantifiable influential factors should be introduced in the empirical model to

TABLE 5 The multiple linear regression results for deflection-type rock avalanches with different landslide scales.

Equations	Volume scale	Intercept	Coefficients				R^2	*p*-value	Comments	MAPE (%)	TIC
			tanα	tanθ	sinγ	$V^{1/3}h^{-1}$					
Eq. 13	Small ($<10^4m^3$)	1.0314	0.7577	0.0717	0.0616	−0.1173	0.96	0.0025	Strong correlation	8.15	0.0550
Eq. 14	Medium (10^4–10^6m^3)	2.9871	0.3808	0.1011	0.0886	−0.2834	0.81	0.026	High correlation	13.59	0.0880
Eq. 15	Large ($\geq10^6m^3$)	2.9084	0.7796	0.0434	0.0854	−0.2241	0.71	0.045	Good correlation	20.72	0.1129

improve the prediction accuracy of large-scale deflection-type rock avalanches.

Empirical models as a practical tool to estimate travel distance can be introduced in the GIS operation platform, which can provide a preliminary delineation of potentially endangered regions of potential rock avalanche (Mergili et al., 2015). This puts forward higher requirements for the accuracy of the prediction models. Although we have verified the validity of the presented empirical model (see Eq. 9) for travel distance prediction of deflected-type rock avalanches triggered by earthquake, there are also some limitations or constraints. On the one hand, the effects of numerous factors, such as ground water, substrate material, stratum lithology, etc., on travel distance were not considered in empirical model. Previous studies have revealed that these factors have a significant impact on the mobility of rock avalanches (e.g., Corominas 1996; Sassa et al., 2004; Guo et al., 2014). For example, due to extensive distribution of groundwater (Zhang et al., 2021), it provides hydrological conditions for the seismic liquefaction of the base material on the movement path, which contributes to the long-distance movement of rock avalanches. Therefore, it deserves more attention that how to quantify these relevant influence factors and incorporate them into the empirical model for travel distance prediction in the future study. On the other hand, in this paper, our database is limited to 54 deflected-type rock avalanches with only seven quantifiable parameters, which might result in wide dispersion and a low coefficient of correlation in some empirical models. Therefore, the next phase of the research focus on a much larger rock avalanche database creation with more quantifiable influential factors, which is conducive to further improve the prediction accuracy of the empirical model.

6 Conclusion

In this study, a database consisting of 54 deflection-type rock avalanches triggered by the Wenchuan earthquake was compiled to obtain a best-fitting empirical model for travel distance prediction. The results indicated that the multiple linear regression of the logarithm of h/L versus the logarithm of other multivariable parameters consisting of slope height (h), landslide volume (V), slope angle (α), deflection angle (θ) and slope transition angle (γ) had a high correlation coefficient and strong statistical significance level. The validity of the proposed empirical model was verified by an independent validation database consisting of 10 deflected-type rock avalanches in the same area. One of the greatest advantages of this empirical model is that all parameters can be quantifiable and obtained before a landslide occurs; thus, this model might be practically applicable in the Wenchuan earthquake area. The results also suggested that the influence of the slope angle (α) on the mobility of rock avalanches was greater than that of the deflection angle (θ) and slope transition angle (γ). However, the influence of local topography on the mobility of large-scale rock avalanches was less than that of small- and medium-scale rock avalanches.

Data availability statement

The original contributions presented in the study are included in the article/Supplementary Material, further inquiries can be directed to the corresponding author.

Author contributions

ZP: Supervision; Project administration; Writing- reviewing and editing. HY: Methodology; Investigation; Writing-original draft preparation. ZH: Investigation; Data-gathering. JL: Investigation; Drafting. XX: Investigation; Data-gathering.

Acknowledgments

We sincerely thank anonymous reviewers for their constructive and valuable suggestions, which help improving this manuscript substantially.

Conflict of interest

The authors declare that the research was conducted in the absence of any commercial or financial relationships that could be construed as a potential conflict of interest.

Publisher's note

References

Armstrong, J. S., and Collopy, F. (1992). Error measures for generalizing about forecasting methods: Empirical comparisons. *Int. J. Forecast* 8, 69–80. doi:10.1016/0169-2070(92)90008-W

Basharat, M., and Rohn, J. (2015). Effects of volume on travel distance of mass movements triggered by the 2005 Kashmir earthquake, in the Northeast Himalayas of Pakistan. *Nat. Hazards* 77, 273–292. doi:10.1007/s11069-015-1590-4

Budetta, P., and De, Riso. R. (2004). The mobility of some debris flows in pyroclastic deposits of the northwestern Campanian region (southern Italy). *Bull. Eng. Geol. Environ*. 63 (4), 293–302. doi:10.1007/s10064-004-0244-7

Chen, L. C., Yang, H. Q., Song, K. L., Huang, W., Ren, X. H., and Xu, H. (2021). Failure mechanisms and characteristics of the Zhongbao landslide at liujing village, wulong, China. *Landslides* 18, 1445–1457. doi:10.1007/s10346-020-01594-1

Corominas, J. (1996). The angle of reach as a mobility index for small and larger landslides. *Can. Geotech. J.* 33, 260–271. doi:10.1139/t96-005

Ding, M. T., and Hu, K. H. (2014). Susceptibility mapping of landslides in Beichuan County using cluster and MLC methods. *Nat. Hazards* 70, 755–776. doi:10.1007/s11069-013-0854-0

Fan, X. M., Hsein, J. C., Janusz, W., Huan, R. Q., Xu, Q., Gianvito, S., et al. (2018). What we have learned from the 2008 wenchuan earthquake and its aftermath: A decade of research and challenges. *Eng. Geol.* 241, 25–32. doi:10.1016/j.enggeo.2018.05.004

Fan, X. Y., Leng, X. Y., and Duan, X. D. (2015). Influence of terrain factor on movement distances of toe-type and turning-type landslides triggered by earthquake. *Chin. J. Rock Soil Mech*. 36, 1380–1388. doi:10.16285/j.rsm.2015.05.021

Finlay, P. J., Mostyn, G. R., and Fell, R. (1999). Landslide risk assessment: Prediction of travel distance. *Can. Geotech. J.* 36, 556–562. doi:10.1139/cgj-36-3-556

Gao, Y., Yin, Y. P., Li, B., Feng, Z., Wang, W. P., and Zhang, N., (2017). Characteristics and numerical runout modeling of the heavy rainfall-induced catastrophic landslide–debris flow at sanxicun, dujiangyan, china, following the wenchuan Ms 8.0 earthquake. *Landslides* 14 (4), 1361–1374. doi:10.1007/s10346-016-0793-4

Ge, Y. F., Tang, H. M., Eldin, M. A. M. Ez., Chen, H. Z., Zhong, P., and Zhang, L., (2019). Deposit characteristics of the Jiweishan rapid long-runout landslide based on field investigation and numerical modeling. *Bull. Eng. Geol. Environ*. 78 (6), 4383. doi:10.1007/s10064-018-1422-3

Ge, Y. F., Zhou, T., Tang, H. M., and Lin, Z. S. (2020a). Influence of the impact angle on the motion and deposition of granular flows. *Eng. Geol.* 275, 105746. doi:10.1016/j.enggeo.2020.105746

Ge, Y. F., Zhou, T., Tang, H. M., and Lin, Z. S. (2020b). Influence of the impact angle on the motion and deposition of granular flows. *Eng. Geol* 275, 105746. doi:10.1016/j.enggeo.2020.105746

Guo, D., Hamada, M., He, C., Wang, Y., and Zou, Y. (2014). An empirical model for landslide travel distance prediction in Wenchuan earthquake area. *Landslides* 11 (2), 281–291. doi:10.1007/s10346-013-0444-y

Hattanji, T., and Moriwaki, H. (2009). Morphometric analysis of relic landslides using detailed landslide distribution maps: Implications for forecasting travel distance of future landslides. *Geomorphology* 103 (3), 447–454. doi:10.1016/j.geomorph.2008.07.009

Heim, A. (1932). *Landslides and human lives*. Vancouver, BC, Canada: Bitech Publishers. 0-921095-06-6.

Hsu, K. J. (1975). Catastrophic debris streams (sturzstroms) generated by rockfalls. *Geol. Soc. Am. Bull.* 86, 1292–2140. doi:10.1130/0016-7606(1975)86<129:CDSSGB>2.0.1

Huang, D., Li, Y. Q., Song, Y. X., Xu, Q., and Pei, X. J. (2019). Insights into the catastrophic xinmo rock avalanche in maoxian county, China: Combined effects of historical earthquakes and landslide amplification. *Eng. Geol.* 258, 105158. doi:10.1016/j.enggeo.2019.105158

Huang, T., Ding, M. T., Tao, S., Tian, S. J., and Yang, J. T. (2017). Numerical simulation of a high-speed landslide in Chenjiaba, Beichuan, China. *J. Mt. Sci*. 14 (11), 2137–2149. doi:10.1007/s11629-017-4516-7

Hungr, O., and Evans, S. G. (2004). Entrainment of debris in rock avalanches: An analysis of a long run-out mechanism. *Geol. Soc. Am. Bull.* 116 (9–10), 1240–1252. doi:10.1130/B25362.1

Hungr, O., Leroueil, S., and Picarelli, L. (2014). The Varnes classification of landslide types, an update. *Landslides* 11, 167–194. doi:10.1007/s10346-013-0436-y

Kang, C., Ren, D. X., Gao, X. F., Han, C. T., and Wang, Y. X. (2021). Study of kinematic characteristics of a rock avalanche and subsequent erosion process due to a debris flow in Wenjia gully, Sichuan, China. *Nat. Hazards* 106, 937–964. doi:10.1007/s11069-021-04501-6

Kang, Y., Zhao, C. Y., Zhang, Q., Lu, Z., and Li, B. (2017). Application of InSAR techniques to an analysis of the guanling landslide. *Remote. Sens*. 9 (10), 1046. doi:10.3390/rs9101046

Knapp, S., and Krautblatter, M. (2020). Conceptual framework of energy dissipation during Disintegration in rock avalanches. *Front. Earth Sci.* 8, 263. doi:10.3389/feart.2020.00263

Leuthold, R. M. (1975). On the use of Theil's inequality coefficients. *Am. J. Agric. Econ*. 57, 344–346. doi:10.2307/1238512

Li, Y., Zhou, R. J., Zhao, G. H., Li, H. B., Su, D. C., and Ding, H. R., (2014). Tectonic uplift and landslides triggered by the wenchuan earthquake and constraints on orogenic growth: A case study from hongchun gully, longmen mountains, sichuan, China. *Quatern. Int*. 349 (28), 142–152. doi:10.1016/j.quaint.2014.05.005

Liu, H. W., Zhao, X. Y., and Xiao, D. (2021a2021). Effects of local topography on the mobility of rock avalanches: A statistical analysis based on 36 cases from south-western China. *Eng. Geol*. 294, 106351. doi:10.1016/j.enggeo.2021.10635

Liu, H. X., Qiu, T., and Xu, Q. (2021b). Dynamic acceleration response of a rock slope with a horizontal weak interlayer in shaking table tests. *PLoS ONE* 16 (4), e0250418. doi:10.1371/journal.pone.0250418

Mergili, M., Krenn, J., and Chu, H-J. (2015). r.randomwalk v1, a multi-functional conceptual tool for mass movement routing. *Geosci. Model Dev.* 8, 4027–4043. doi:10.5194/gmd-8-4027-2015

Mitchell, A., McDougall, S., Nolde, N., BrideauWhittall, M. A. J., and Aaron, J. B. (2020). Rock avalanche runout prediction using stochastic analysis of a regional dataset. *Landslides* 17, 777–792. doi:10.1007/s10346-019-01331-3

Qiu, H. J., Cui, P., Hu, S., Regmi, A. D., Wang, X. G., and Yang, D. D. (2018). Developing empirical relationships to predict loess slide travel distances: A case study on the loess plateau in China. *B. Eng. Geol. Environ*. 77, 1299–1309. doi:10.1007/s10064-018-1328-0

Sassa, K., Wang, G. H., Fukuoka, H., Wang, F. W., Ochiai, T., and Sugiyama, M. (2004). Landslide risk evaluation and hazard zoning for rapid and long-travel landslides in urban development areas. *Landslides* 1, 221–235. doi:10.1007/s10346-004-0028-y

Strom, A. L., Li, L., and Lan, H. (2019). Rock avalanche mobility: Optimal characterization and the effects of confinement. *Landslides* 16, 1437–1452. doi:10.1007/s10346-019-01181-z

Tang, C., van Asch, T. W. J., Chang, M., Chen, G. Q., Zhao, X. H., and Huang, X. C. (2012). Catastrophic debris flows on 13 august 2010 in the qingping area, southwestern China: The combined effects of a strong earthquake and subsequent rainstorms. *Geomorphol* 139–140, 559–576. doi:10.1016/j.geomorph.2011.12.021

Wang, H., Ran, Y. K., Li, Y. B., Gomez, F., and Chen, L. C. (2014). Southwest China is on the southeastern edge of the Tibetan Plateau and is characterised by complex geological structures. *Tectonophysics* 628, 206–217. doi:10.1016/j.tecto.2014.04.040

Yang, J. Q., Xu, Z. M., Zhang, R., Chen, J. P., Ren, Z., and Luo, R. Z., (2017). Formation and evolution of Emeishan basalt saprolite in vadose zones of Touzhai landslide source Rockmass. *J. Mt. Sci.* 14 (6), 1174–1184. doi:10.1007/s11629-016-4169-y

Zhan, W. W., Fan, X. M., Huang, R. Q., Pei, X. J., Xu, Q., and Li, W. L. (2017). Empirical prediction for travel distance of channelized rock avalanches in the Wenchuan earthquake area. *Nat. Hazards Earth Syst. Sci*. 17, 833–844. doi:10.5194/nhess-17-833-2017

Zhang, M., Yin, Y., and McSaveney, M. (2016). Dynamics of the 2008 earthquake-triggered wenjiagou creek rock avalanche, qingping, sichuan, China. *Eng. Geol.* 200, 75–87. doi:10.1016/j.enggeo.2015.12.008

Zhang, M., and Yin, Y. P. (2013). Dynamics, mobility-controlling factors and transport mechanisms of rapid long-runout rock avalanches in China. *Eng. Geol.* 167, 37–58. doi:10.1016/j.enggeo.2013.10.010

Zhang, Y. H., Dai, Y. S., Wang, Y., Huang, X., Xiao, Y., and Pei, Q. M. (2021). Hydrochemistry, quality and potential health risk appraisal of nitrate enriched groundwater in the Nanchong area, southwestern China. *Sci. Total Environ.* 784, 147186. doi:10.1016/j.scitotenv.2021.147186

Zhang, Y. H., Yao, R. W., Wang, Y., Duo, J., and Cao, H. W. (2022). Zircon U–Pb and sericite Ar–Ar geochronology, geochemistry and S–Pb–Hf isotopes of the Zebuxia Pb–Zn deposit, Tibet, southwestern China. *Ore Geol. Rev.* 148, 104999. doi:10.1016/j.oregeorev.2022.104999

Zheng, G., Xu, Q., and Peng, S. Q. (2018). Chute experiments of the long-runout distance of rock avalanche (in Chinese). *Rock Soil Mech.* 40 (12), 1–10. doi:10.16285/j.rsm.2018.1827